Oncogene (2015) **34,** 978–985
© 2015 Macmillan Publishers Limited All rights reserved 0950-9232/15
www.nature.com/onc

ORIGINAL ARTICLE

Contributions of DNA repair, cell cycle checkpoints and cell death to suppressing the DNA damage-induced tumorigenic behavior of *Drosophila* epithelial cells

A Dekanty[1,3,4], L Barrio[1,3] and M Milán[1,2]

When exposed to DNA-damaging agents, components of the DNA damage response (DDR) pathway trigger apoptosis, cell cycle arrest and DNA repair. Although failures in this pathway are associated with cancer development, the tumor suppressor roles of cell cycle arrest and apoptosis have recently been questioned in mouse models. Using *Drosophila* epithelial cells that are unable to activate the apoptotic program, we provide evidence that ionizing radiation (IR)-induced DNA damage elicits a tumorigenic behavior in terms of E-cadherin delocalization, cell delamination, basement membrane degradation and neoplasic overgrowth. The tumorigenic response of the tissue to IR is enhanced by depletion of *Okra/DmRAD54* or *spnA/DmRAD51*—genes required for homologous recombination (HR) repair of DNA double-strand breaks in G2—and it is independent of the activity of Lig4, a ligase required for nonhomologous end-joining repair in G1. Remarkably, depletion of *Grapes/DmChk1* or *Mei-41/dATR*—genes affecting DNA damage-induced cell cycle arrest in G2—compromised DNA repair and enhanced the tumorigenic response of the tissue to IR. On the contrary, DDR-independent lengthening of G2 had a positive impact on the dynamics of DNA repair and suppressed the tumorigenic response of the tissue to IR. Our results support a tumor suppressor role of apoptosis, DNA repair by HR and cell cycle arrest in G2 in simple epithelia subject to IR-induced DNA damage.

Oncogene (2015) **34,** 978–985; doi:10.1038/onc.2014.42; published online 17 March 2014

INTRODUCTION

Cells and tissues are continuously exposed to extrinsic and intrinsic insults that generate DNA damage including ultraviolet and ionizing radiation (IR) as well as reactive oxygen species produced during normal cellular metabolism. In order to lessen the detrimental effects of DNA lesions, the conserved ataxia telangiectasia-mutated (ATM)/Chk2 and ataxia telangiectasia-related (ATR)/Chk1 kinase pathways are rapidly activated in response to DNA damage and phosphorylate numerous substrates involved in DNA repair, cell cycle arrest and/or apoptosis (reviewed in Negrini *et al.*[1]). The conserved tumor suppressor protein p53 is a major downstream effector of the DNA damage response (DDR) pathway. p53 is phosphorylated by ATM/Chk2 and has a critical role in driving cell cycle arrest or apoptosis; these processes are mediated mainly by the transcriptional upregulation of *p21* or the pro-apoptotic genes *Puma* and *Noxa*, respectively (reviewed in Lane and Levine[2]). The DDR machinery has crucial roles during development and tissue homeostasis, as mutations in DDR genes lead to developmental defects, genetic diseases, premature aging and cancer (reviewed in Halazonetis *et al.*[3] and Jackson and Bartek[4]). Mutations in DNA repair genes have been identified in hereditary cancer, whereas mutations in *p53* and *ATM* are frequently associated with sporadic (nonhereditary) cancers. It has been generally accepted that tumorigenesis is blocked by p53-mediated cell cycle arrest, apoptotic cell death and/or cellular senescence. However, new data revealed unpredicted tumor suppressor activity of p53. DNA damage-induced tumorigenesis is suppressed in mice bearing mutant forms of p53 that are unable to induce apoptosis[5,6] or both apoptosis and cell cycle arrest.[7] Furthermore, the combined loss of p53-mediated cell cycle arrest, senescence and apoptosis is not sufficient to abrogate the tumor suppression activity of p53, and mice mutant for p21 and the pro-apoptotic genes *Puma* and *Noxa* remain tumor free in contrast to p53-deficient mice.[6,8] These results indicate that the tumor suppressor activity of p53 might also rely on its capacity to coordinate DNA repair and regulate metabolism, and they question the classical contributions of cell cycle arrest and apoptosis to suppressing spontaneous tumorigenesis.

The imaginal discs of *Drosophila*, simple monolayered epithelia that grow about a thousand-fold in mass and cell number during larval development, are valuable models in which to dissect the molecular and cellular mechanisms underlying tumor initiation and progression.[9–12] *Drosophila* is a very attractive model in which to analyze the contributions of cell cycle arrest and apoptosis to suppressing DNA damage-induced tumorigenesis, as both cell proliferation and programmed cell death can be easily manipulated in a DDR-independent manner, and both DNA damage-induced cell cycle arrest and apoptosis are independently controlled by ATM and ATR and their targets (reviewed in Song[13]). Although ATM downstream targets Chk2 and Dp53 regulate the immediate apoptotic response of the tissue to IR,[14,15] cell cycle arrest in G2 is controlled by the activity of *Drosophila* ATR (dATR),[16] and its downstream target DmChk1.[17] Repair of double-strand breaks (DSBs) is mediated in G2 by an error-free

[1]Institute for Research in Biomedicine (IRB Barcelona), Barcelona, Spain and [2]Institució Catalana de Recerca i Estudis Avançats (ICREA), Barcelona, Spain. Correspondence: Professor M Milán, Department of Cell and Development Biology, Institute for Research in Biomedicine (IRB Barcelona), Baldiri Reixac, 10-12, Barcelona 08028, Spain.
E-mail: marco.milan@irbbarcelona.org
[3]These authors contributed equally to this work.
[4]Current address: Instituto de Agrobiotecnología del Litoral, Facultad de Bioquímica y Ciencias Biológicas, Universidad Nacional del Litoral, 3000 Santa Fe, Argentina.
Received 26 September 2013; revised 4 February 2014; accepted 7 February 2014; published online 17 March 2014

mechanism called homologous recombination (HR), and in G1 by an error-prone mechanism called nonhomologous end-joining (NHEJ). Whereas DmRAD51 and the DEAD-like helicase DmRAD54 have essential roles in HR,[18,19] NHEJ is executed by the activity of the ATP-dependent DNA ligase Lig4.[20]

Here we studied the potential protumorigenic action of IR-induced DNA damage and the contribution of cell cycle arrest, apoptosis and DNA repair to tumor progression. We first show that *Drosophila* epithelial cells subject to IR and unable to activate the apoptotic program at the level of the pro-apoptotic genes or the effector Caspases Drlce and Dcp1 present a tumorigenic behavior in terms of E-cadherin delocalization, cell delamination, cell motility, basement membrane degradation and expression of the mitogenic molecule Wingless (Wg). We also unravel a G2-specific role of cell cycle arrest and DNA repair in suppressing IR-induced tumorigenesis. Our results reinforce the suppressor activities of DNA repair, cell cycle arrest and apoptosis in IR-induced tumor initiation in simple epithelia. Whereas p53-dependent DNA repair might be sufficient to counteract the tumorigenic action of the DNA damage produced under normal physiological conditions, cell cycle arrest and apoptosis might enter into action only upon induction of nonphysiological levels of DNA damage.

RESULTS

Tumorigenic behavior of IR-induced delaminating cells

When IR-treated cells are maintained in the tissue by means of expression of the baculovirus protein P35, which binds and represses the activity of effector caspases Drlce and Dcp1 and blocks cell death,[21] or by expressing a double-stranded RNA (dsRNA) form of the effector caspase Drlce, ectopic expression of the mitogenic molecule Wg is observed (white arrows in Figures 1b–d).[22] Note that transgene expression is restricted to one compartment of the wing disc and the neighboring compartment serves as control (Figures 1b–d). Ectopic expression of Wg is dependent on the activity of the Jun N-terminal kinase (JNK) pathway, as co-expression of a dominant-negative version of *Drosophila* JNK (Basket^{DN}) together with p35 rescues Wg expression (Figure 1f). Remarkably, JNK-dependent expression of Wg also causes a clear overgrowth of the IR-treated tissue expressing p35. Thus, the p35-expressing territory (the P compartment) is enlarged when compared with the neighboring one (the A compartment), and this enlargement is fully reversed by co-expression of Basket^{DN} (Figure 1l). These observations prompted us to analyze the potential protumorigenic action of the IR treatment.

The wing primordium is a cellular monolayer that forms a two-sided epithelial sac and consists of two apposed epithelia: the main epithelium that is pseudostratified and the peripodial membrane that is squamous (Figure 1a). The apical (ap) side of both epithelia faces the lumen and the basal (bs) side is located at the periphery. We noted that the ectopic expression of Wg upon IR was restricted to small groups of delaminated cells located on the basal side of the main epithelium (Figures 1h and i), thus unraveling a neoplastic response of the tissue to this radiation. Interestingly, clones of cells mutant for the pro-apoptotic genes *hid*, *reaper* and *grim* (in *Df(H99)* clones) also delaminated upon IR and induced JNK activation, monitored by the expression of Wg (Figures 1e and j). This observation implies that delamination and JNK activation are not a consequence of entry into apoptosis. Delamination was not caused by JNK activation either as IR-treated wing discs expressing p35 and a dominant-negative version of JNK (Basket^{DN}) showed delaminated cells on the basal side of the epithelium that did not express Wg (Figure 1k).

Epithelial architecture relies on the polarization of the plasma membrane into apical and basolateral domains separated by adherens junctions, and genetic depletion of components of the Cdc42/Par6/atypical protein kinase C or Scribbled/Disc Large/Lgl polarity complexes induces a reduction in junctional DE-cadherin (DE-cad) level, cell delamination and JNK activation.[9,23–25] We then used antibodies against Atypical Protein Kinase C, Disc Large and DE-cad to view the subapical, basolateral and junctional domains, respectively, in IR-induced delaminating cells (Figure 2a). Atypical Protein Kinase C and Disc Large remained at the membrane of these cells (Figure 2b, b′). However, their overall protein levels

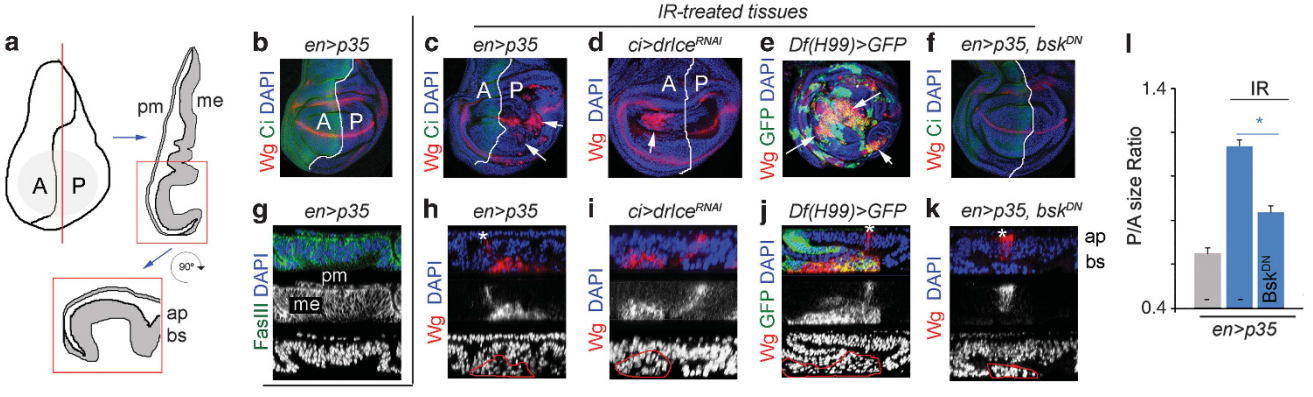

Figure 1. Cell delamination and Wg expression are not caused by entry into apoptosis. (**a**) Cartoon depicting the wing primordium (left), a cross-section along the red line (right) and a magnification of the region within the red square (bottom). Whereas the main epithelium (me) is pseudostratified, the peripodial membrane (pm) is a squamous epithelium. Anterior (A) and posterior (P) compartments, and apical (ap) and basal (bs) sides of the main epithelium are depicted. (**b**–**f**) Wing primordia from wild-type (**b**), *en-gal4; UAS-p35* (**c**), *ci-gal4; UAS- Drlce^{RNAi}* (**d**), *en-gal4; UAS-p35; UAS-bsk^{DN}* (**f**) larvae or with clones of cells mutant for *Df(H99)* and expressing green fluorescent protein (GFP; green, **e**), subject to IR 72 h before dissection and stained for Wg (red), Ci (green, **b**, **c**, **f**), and DAPI (blue). *en-gal4* (**b**, **c**, **f**) and *ci-gal4* (**d**) drive transgene expression in the posterior (P) and anterior (A) compartments, respectively. Ci labels the A compartment in **b**, **c** and **f**. White arrows in **a**–**c** point to Wg-expressing cells. (**g**–**k**) Cross-sections of wing primordia from wild-type (**g**), *en-gal4; UAS-p35* (**h**), *ci-gal4; UAS- Drlce^{RNAi}* (**i**), *en-gal4; UAS-p35; UAS-bsk^{DN}* (**k**) larvae or with clones of cells mutant for *Df(H99)* and expressing GFP (green, **j**), subject to IR 72 h before dissection and stained for Fas III (green, **g**), Wg (red, **h**–**k**) and DAPI (blue). The endogenous expression of Wg is marked by an asterisk and delaminated cells by a red line. The apical (ap) and basal (bs) sides of the epithelium are indicated. In **g**, the peripodial membrane (pm) and main epithelium (me) are indicated. (**l**) Histogram plotting the P/A size ratio of wing primordia expressing p35 and the indicated transgenes and quantified 72 h after IR treatment. Error bars represent s.e.m. $^*P < 0.001$.

© 2015 Macmillan Publishers Limited

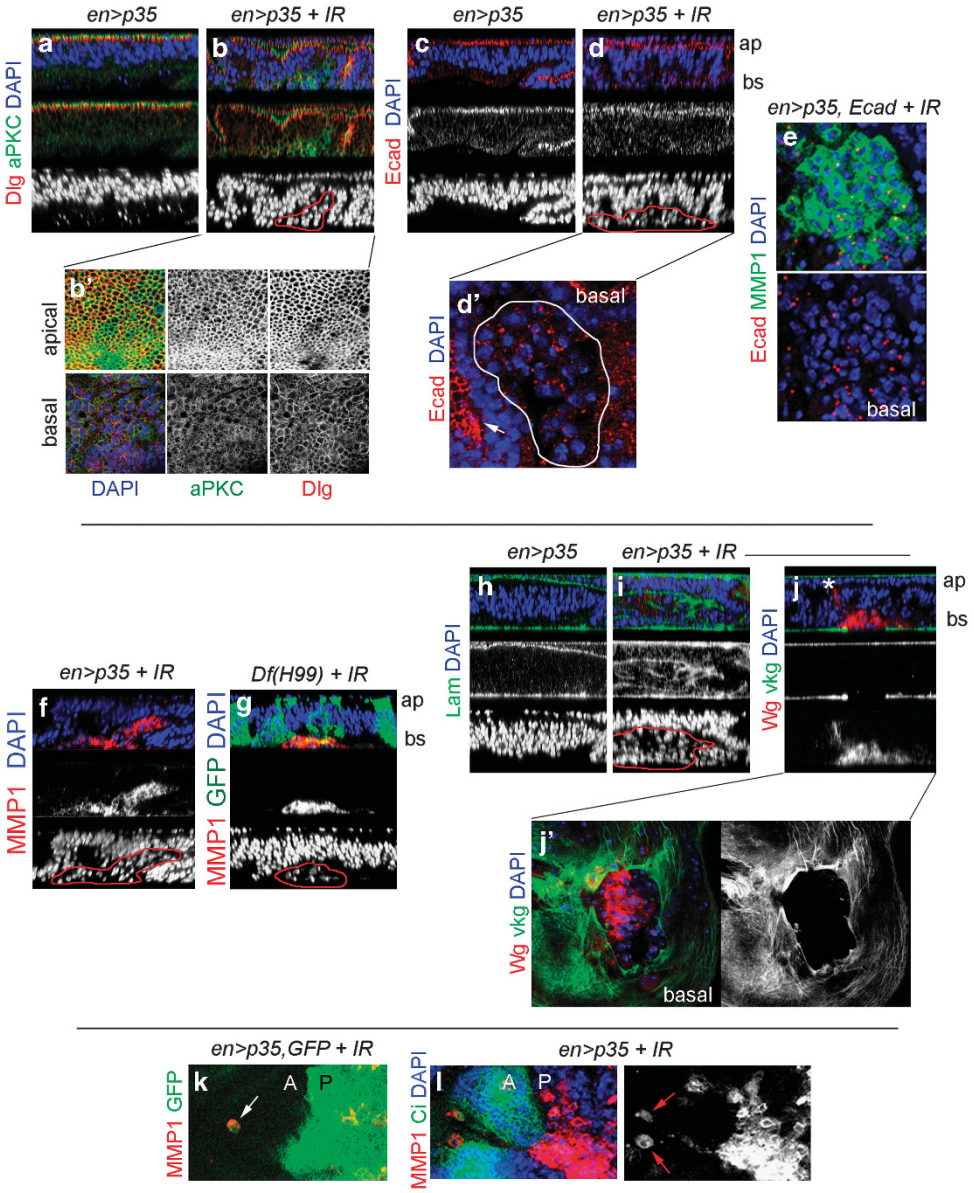

Figure 2. Tumorigenic behavior of IR-induced delaminated cells. (**a-d**) Cross-sections of the posterior compartment of wing primordia expressing the indicated transgenes under the control of the *en-gal4* driver and stained for Dlg (Disc Large; red, **a**, **b**), atypical protein kinase C (aPKC; green, **a**, **b**), E-cad (red, **c**, **d**) and DAPI (blue). In **b** and **d**, larvae were subjected to IR 72 h before dissection. Apical (ap) and basal (bs) sides of the epithelium are indicated. (**b**, **d′**) X-Y sections of the apical or basal sides of the wing epithelia are shown in **b** and **d**. In **d′**, delaminated cells are marked by a white line, and the nondelaminated tissue by an arrow. (**e**) X-Y sections of the basal side of a wing epithelium expressing the indicated transgenes, subject to IR 72 h before dissection and stained for E-cad (red), MMP1 (green) and DAPI (blue). (**f**–**j**) Cross-sections of the posterior compartment of wing primordia expressing the indicated transgenes under the control of the *en-gal4* driver (**f**, **h**–**j**) or with clones of cells mutant for *Df(H99)* and expressing green fluorescent protein (GFP; green, **g**) and stained for MMP1 (red, **f**, **g**), Wg (red, **j**), DAPI (blue), laminin-γ (labels the basement membrane (BM) in green, **h**, **i**), and *viking-GFP* (*collagen IV*, green, **j**). In **f**, **g**, **i** and **j**, larvae were subject to IR 72 h before dissection. In **j**, the endogenous expression of Wg is marked by an asterisk. Apical (ap) and basal (bs) sides of the epithelium are indicated. (**j′**) X-Y section of the basal side of the wing epithelium is shown in **j**. (**e**, **k**, **l**) X-Y sections of the basal side of wing primordia expressing the indicated transgenes, subject to IR 72 h before dissection and stained for MMP1 (red), Ci (green, **l**) and DAPI (blue). *en-gal4* drives transgene expression in the posterior (P) compartment and the anterior (A) compartment is labeled by the expression of Ci in **l**. Note in **k** and **l**, the presence of delaminated cells (arrows) originating from the P compartment and migrating toward the nearby A compartment.

were severely reduced (Figure 2b′, bottom panels), when compared with nondelaminated cells (Figure 2b′, top panels). Interestingly, DE-cad lost its tight junctional distribution, and the overall protein levels were clearly decreased in delaminated cells (Figures 2c, d and d′). This molecule was no longer detectable in most of the delaminated cells, with the exception of some small discrete puncta. Overexpression of a modified version of DE-cad (DE-cadΔCyt:α-catenin), able to rescue the adhesion properties of *E-cad*-mutant cells and unable to interfere with endogenous β-catenin signaling,[26] did not block the delamination process, and the overexpressed form of DE-cad also localized to small discrete puncta in delaminating cells (Figure 2e). Thus, dissociation

© 2015 Macmillan Publishers Limited

of *Drosophila* epithelial cells upon IR is not due to reduced levels of DE-cad but is most probably caused by DE-cad mis-localization. Interestingly, delaminating cells expressed Matrix Metalloproteinase 1 (MMP1; Figures 2e–g), and MMPs are known to contribute to basement membrane degradation in flies and mammals.[25,27,28] Consistently, the basement membrane, labeled with Laminin-γ or with a GFP (green fluorescent protein)-tagged protein trap in the *viking/collagen IV* gene, was disrupted in the delaminated cell population (Figures 2h–j, j′). MMP1-expressing delaminated cells also became motile and were observed in the nearby compartment (Figures 2k and l). Altogether, these results unveil a tumorigenic response of the tissue to IR upon additional blockade of the apoptotic pathway.

A tumor suppressor role of HR repair of DSBs

As entry into apoptosis is not required for IR-induced activation of JNK, we next addressed whether the induction of DSBs by IR treatment contributed to JNK activation and to the tumorigenic behavior of the tissue. The DNA damage sensor ATM recruits and phosphorylates the histone H2A variant, H2AX, to mark the sites of damage (reviewed in Srivastava *et al.*[29]). We observed elevated levels of phosphorylated H2Av (P-H2Av), the functional homolog of H2AX in *Drosophila*, in wild-type wing discs subject to IR and dissected 5 h after (Supplementary Figure S1). Overall, P-H2Av levels decreased 72 h after the IR treatment (Supplementary Figure S1). dATR/Mei-41 kinase is a conserved regulator of cellular responses to DSBs and has been reported to phosphorylate H2Av during the repair of meiotic DSBs.[30] Depletion of this kinase (by means of expression of a dsRNA form of *mei-41*) also reduced P-H2Av levels in IR-treated wing discs (Figure 3b), thus supporting a general role of Mei-41 in the repair of IR-induced DSBs. In wing discs expressing p35, the dynamics of H2Av phosphorylation upon IR were largely similar to that observed in control wing discs, with the exception of small groups of cells with elevated levels of P-H2Av up to 72 h after IR (red arrows in Figure 3a). Thus, apoptosis inhibition does not have a major impact on the dynamics of DSB repair.

In order to analyze the causal relationship between IR-induced DNA damage, monitored by P-H2Av and JNK activation, we compromised the repair of DSBs and analyzed the impact of wing discs subjected to IR and expressing p35 on JNK activation and tissue overgrowth. DSB repair is mediated by two distinct mechanisms. On one hand, an error-free mechanism, HR, executed by the activities of DmRAD51/spnA[18] and the DEAD-like helicase DmRAD54/Okra,[19] allows a damaged chromosome to be repaired using a sister chromatid available in S/G2. On the other hand, NHEJ, executed by the activity of Lig4,[20] takes place in G1 and induces error-prone repair. We then compared the contributions of these two DNA repair mechanisms with the IR-induced tumorigenic behavior of the tissue. Although depletion of DmRAD54/Okra or DmRAD51/spnA maintained the overall high levels of P-H2Av observed immediately after IR treatment during at least 72 h (Figures 3c–e and Supplementary Figure S1, compared with Figure 3a), the impact of Lig4 depletion on P-H2Av dynamics was undetectable (Figure 3f and Supplementary Figure S1). Similar results were obtained with an independent dsRNA form of DmRAD54/Okra (Supplementary Figure S3). These observations indicate that HR makes a greater contribution to DSB repair after IR treatment than NHEJ. Interestingly, the levels of JNK activation, the number of delaminating cells and the degree of tissue overgrowth induced by IR were increased in DmRAD54/Okra-depleted tissues (Figures 3g, h and l), and the resulting IR-induced tissue overgrowth was fully rescued upon depletion of the JNK pathway (Figures 3i and l). A similar impact on JNK activation was observed in DmRAD51/spnA-depleted tissues (Figure 3j and Supplementary Figure S3). JNK was not activated in untreated tissues depleted of DmRAD54/Okra or DmRAD51/spnA and expressing p35 (Supplementary Figure S2). Consistent with the observation that Lig4 had no impact on the P-H2Av dynamics of IR-treated tissues, JNK activation and the degree of tissue overgrowth induced by IR was very similar in control and *lig4*-mutant wing discs expressing p35 (Figures 3k and l). Taken together, these results support the notion that IR-induced DSBs contribute to JNK activation and reveal a tumor suppressor role of error-free HR repair of DNA DSBs.

A tumor suppressor role of cell cycle arrest in G2

The G2 cell cycle arrest induced by IR is controlled in *Drosophila* by the activity of dATR/Mei-41 (Song *et al.*[16]) and its downstream target DmChk1 (Grapes in *Drosophila*)[17] and is thought to contribute to the repair of DSBs by HR. Consistently, depletion of DmChk1/Grapes maintained the overall high levels of P-H2Av observed immediately after IR treatment during at least 72 h (Figures 4a and b, compared with Figure 3a). Interestingly, the overall levels of JNK activation and the resulting overgrowth of the DmChk1/Grapes tissue were increased when compared with control samples (Figures 4c–e). An even stronger impact on JNK activation and tissue overgrowth was observed upon depletion of dATR/Mei-41 levels (Figures 4c, d and f; expression of the JNK targeted *puc* is shown in Figure 4f), most probably because this kinase is also directly involved in DSB repair.[16] A similar enhancement of JNK activation was observed upon depletion of DmChk1/Grapes or dATR/Mei-41 with independent dsRNA forms (Supplementary Figure S3). The resulting tissue overgrowth was fully rescued upon depletion of the JNK pathway (Figures 4c and g) and JNK was not activated in untreated tissues depleted of DmChk1/Grapes or dATR/Mei-41 and expressing p35 (Supplementary Figure S2). These results unravel a tumor suppressor role of IR-induced cell cycle arrest in G2 and support the notion that this cell cycle arrest contributes to the repair of DSBs by HR.

In order to further characterize the tumor suppressor role of IR-induced cell cycle arrest in G2, we addressed whether DDR-independent lengthening of G2 contributed to HR-dependent repair of DSBs, and whether this lengthening had any impact on the level of JNK activation. Tribbles is an ubiquitin ligase that binds, ubiquitinates and degrades String, the Cdc25 *Drosophila* ortholog involved in activating Cdc2 and promoting the G2/M transition.[31–34] Tribbles overexpression in epithelial cells is well known to induce a G2 lengthening and a concomitant shortening of G1 to maintain the overall length of the cell cycle.[34] Interestingly, Tribbles overexpression in IR-treated wing discs caused a mild but reproducible reduction in the overall levels of P-H2Av (Figure 4h) and suppressed JNK activation (Figures 4i and j, compared with Figures 4d and e). Similar results were obtained upon expression of dsRNA forms of *string* or *cdc2* (Figure 4k and data not shown).

Overexpression of the CDK inhibitor Dacapo (Dap, the *Drosophila* p21/p27 ortholog), which traps the cyclin E/CDK2 complex in a stable but inactive form,[36,37] induces G1 lengthening in epithelial cells and a concomitant shortening of G2 to maintain the overall length of the cell cycle.[35] In this case, repair of IR-induced DSBs might be compromised, given that the contribution of NHEJ, which takes place in G1, to DNA repair is minor with respect to HR, which takes place in G2 (Figure 3). Consistent with this proposal, Dacapo overexpression in IR-treated tissues maintained the overall high levels of P-H2Av observed immediately after IR treatment during at least 72 h (Figures 4l and m), and increased the levels of IR-induced JNK activation (Figures 4n and o, compared with Figures 4d and e). These results reinforce the relative contributions of NHEJ and HR to the repair of IR-induced DSBs and to the suppression of IR-induced JNK activation.

© 2015 Macmillan Publishers Limited

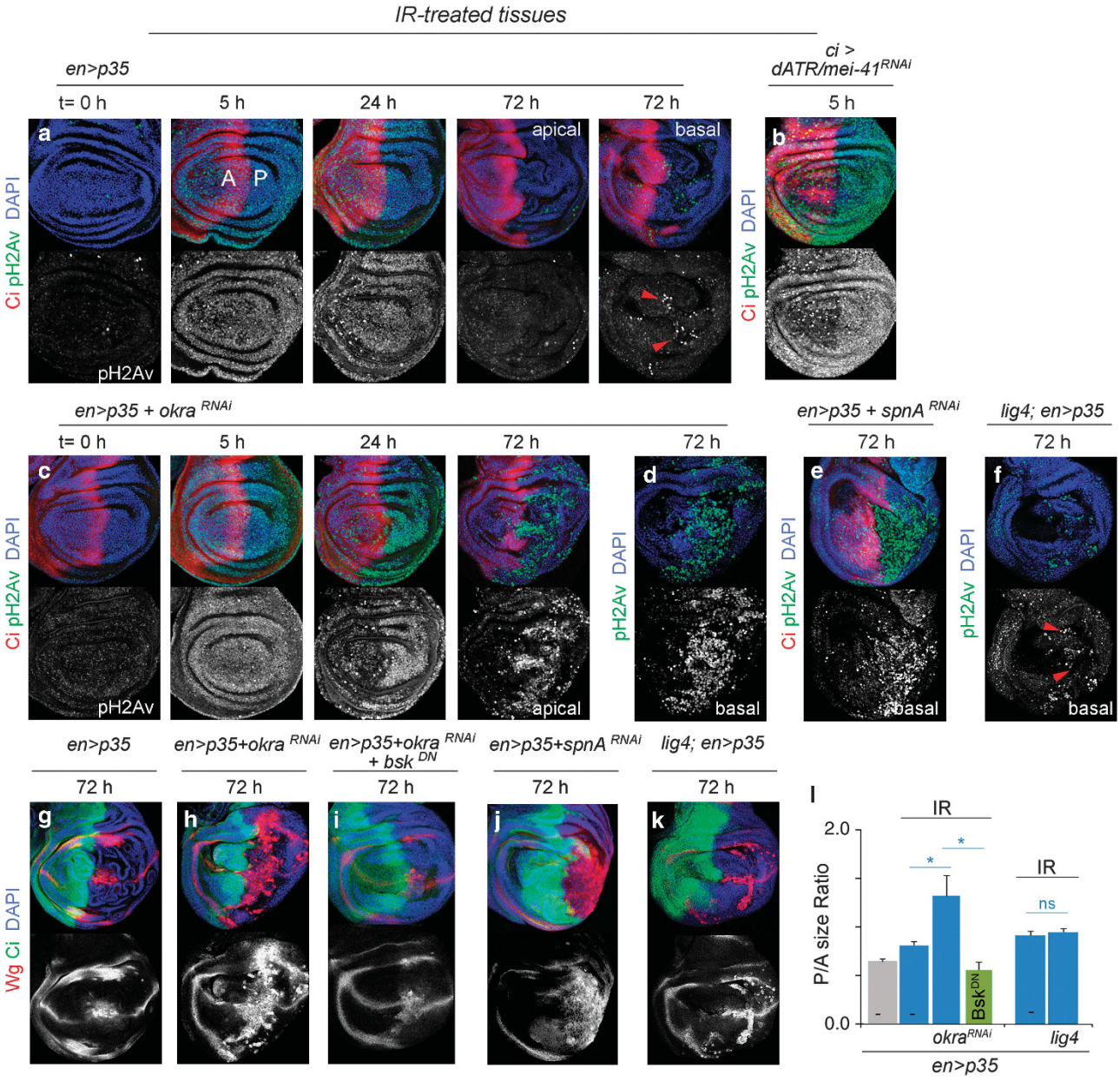

Figure 3. A tumor suppressor role of HR DNA repair. (**a**–**k**) Wing primordia expressing the indicated transgenes under the control of the *en-gal4* (**a**, **c**–**k**) or *ci-gal4* (**b**) drivers and stained for pH2Av (green or white, **a**–**f**), Wg (red, g–k), Ci (red in **a**–**c** and **e**; green in **g**–**k**) and subjected to IR at the indicated time points before dissection. *en-gal4* and *ci-gal4* drive transgene expression in the posterior (P) compartment and anterior (A) compartments, respectively. Ci expression labels the A compartment. The basal side of the epithelium is shown in panels **d**–**f**. In the other panels, the apical side is shown. Red arrowheads, in **a** and **f**, point to pH2Av-positive cells localized on the basal side of the epithelium. (**l**) Histogram plotting the P/A size ratio of wing primordia subject to IR 72 h before dissection and expressing the indicated transgenes under the control of the *en-gal4* driver. Error bars represent s.e.m. $*P < 0.001$. NS, not statistically significant.

DISCUSSION

DNA damage-induced tumorigenesis

Here we have used the imaginal discs of *Drosophila* to revisit the contributions of DNA repair, cell cycle arrest and apoptosis in suppressing DNA damage-induced tumorigenesis. The tumorigenic behavior of the tissue to IR-induced DNA damage relies on groups of cells losing their apical-basal polarity, mislocalizing DE-cad, delaminating from the main epithelium, becoming motile, and activating the stress-responsive JNK pathway, which drives a transcriptional program that induces the expression of the mitogenic molecule Wg and MMP1. The tumorigenic response of the tissue to IR-induced DNA damage was unraveled upon inhibition of the apoptotic program at various levels, including the pro-apoptotic genes and the effector caspases. Thus, cell delamination and JNK activation is not a consequence of the entry into apoptosis. The contribution of NHEJ to the repair of IR-induced DSBs was undetectable and IR-induced JNK activation and tumorigenesis were largely unaffected by mutations in *lig4*. On the contrary, HR had a major role in the repair of these DSBs, and depletion of elements involved in HR had a major impact on the tumorigenic behavior of the tissue. Consistent with the role of HR in DSB repair, which occurs in S/G2, we unveiled a tumor suppressor role of the cell cycle arrest in G2 upon IR-induced DNA damage. Thus, defects in G2 cell cycle arrest upon IR treatment

© 2015 Macmillan Publishers Limited

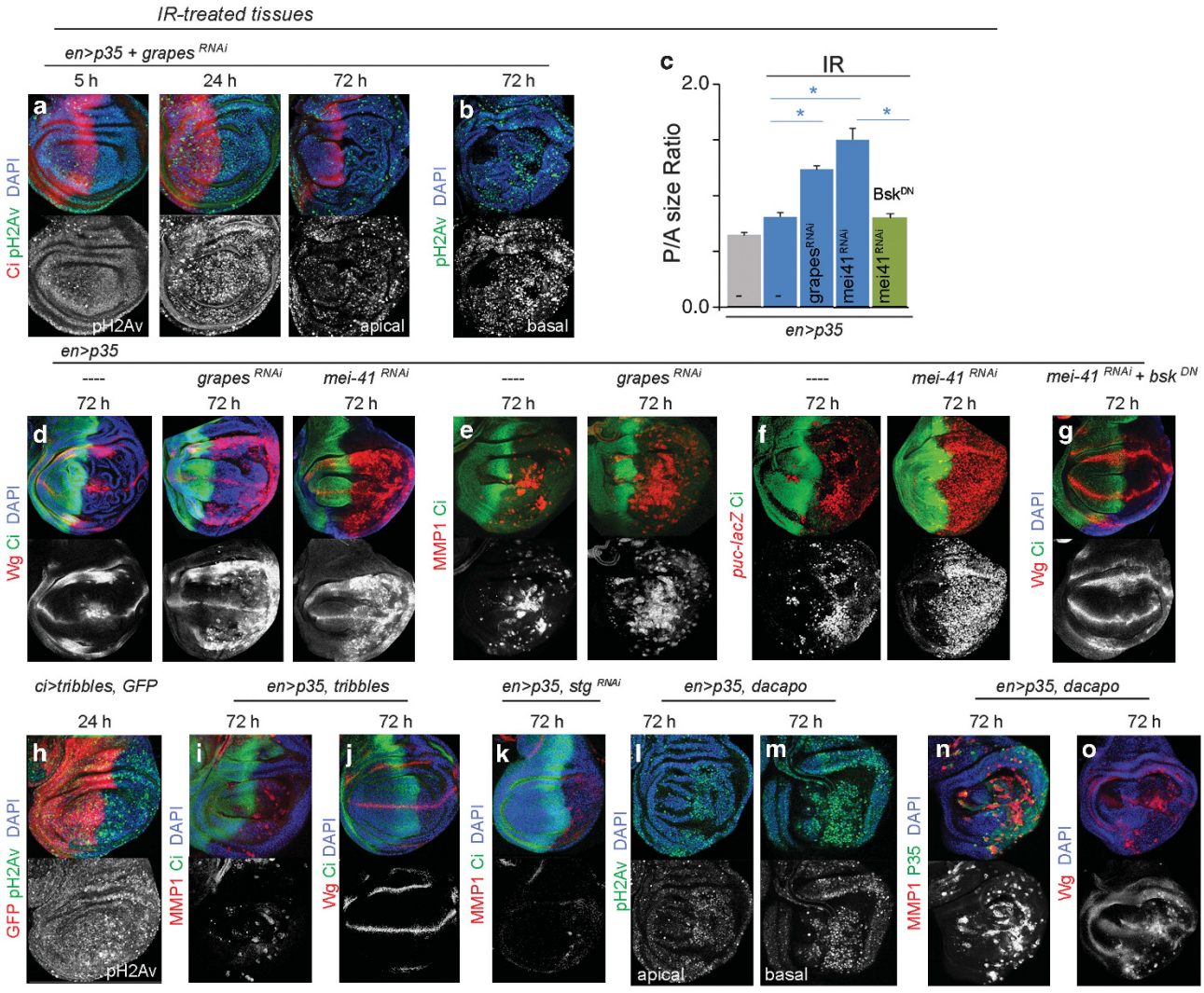

Figure 4. A tumor suppressor role of cell cycle arrest in G2. (**a**, **b**, **d**–**o**) Wing primordia expressing the indicated transgenes, stained for pH2Av (green or white, **a**, **b**, **h**, **l**, **m**), Ci (red in **a**; green in **d**–**g**, **i**–**k**), DAPI (blue in **a**, **b**, **d**, **g**–**o**), Wg (red, **d**, **g**, **j**, **o**), MMP1 (red, **e**, **i**, **k**, **n**), *puckered-lacZ* (red, **f**), green fluorescent protein (GFP; red, **h**), P35 (green in **n**) and subjected to IR 72 h before dissection. *en-gal4* and *ci-gal4* drive transgene expression in the posterior (P) compartment and anterior (A) compartment, respectively. Ci expression labels the A compartment. (**c**) Histogram plotting the P/A size ratio of wing primordia subject to IR 72 h before dissection and expressing, under the control of the *en-gal4* driver, the indicated transgenes. Error bars represent s.e.m. $^{*}P < 0.001$.

compromised the dynamics of DNA repair and enhanced the tumorigenic response of the tissue. Remarkably, DDR-independent lengthening of G2 contributed to DNA repair and completely rescued IR-induced JNK activation. These results support the proposal that IR-induced G2 cell cycle arrest contributes to the repair of DSBs by HR. Taken together, our observations reinforce the classical contributions of apoptosis, cell cycle arrest and DNA repair to suppressing IR-induced tumorigenesis, and provide an ideal genetic experimental setup to identify new molecular elements involved in DNA damage-induced tumorigenesis.

Whereas apoptosis and cell cycle arrest have a major role in suppressing IR-induced tumorigenesis, they are dispensable for p53-dependent suppression of spontaneous tumor development. Thus, mice mutant for *p21* and the pro-apoptotic genes *Puma* and *Noxa* remain tumor free, in contrast to DDR or *p53*-mutant mice, and the combined loss of p53-mediated cell cycle arrest, senescence and apoptosis is not sufficient to abrogate the tumor suppression activity of p53.[8,38] These results imply that p53-dependent DNA repair might be sufficient to counteract the tumorigenic action of the DNA damage produced under normal physiological conditions, and cell cycle arrest and apoptosis might enter into action only upon induction of nonphysiological levels of DNA damage.

Genomic instability and tumorigenesis

We observed a temporal delay between the overall levels of H2Av phosphorylation, which mark the presence of DSBs, and the induction of JNK activity in IR-treated tissues expressing p35. Thus, JNK activation was still observed 72 h after the IR treatment, a time at which P-H2Av levels were very low. We also noted that DSBs were observed throughout the *DmRAD54/okra-*, *DmRAD51/spnA-* or *DmChk1/grapes*-depleted tissues in both delaminated and non-delaminated cells, while sustained JNK activation was restricted only to delaminated cells. These observations suggest that JNK activation is an indirect consequence of the presence of DSBs in the tissue. Impaired HR repair of DSBs, caused by *DmRAD54/okra* or *DmRAD51* depletion, enhances JNK activation in IR-treated tissues (Figures 3h and j and Supplementary Figure S3) and has been previously shown in *Drosophila* tissues to induce genome rearrangements such as deletions.[39,40] Thus, genome rearrangements, generated by imprecise repair of DSBs, might contribute to

© 2015 Macmillan Publishers Limited

JNK-mediated tumorigenesis of IR-treated tissues expressing p35. Consistent with this proposal, the molecular and cellular mechanisms underlying the tumor-like behavior induced by the IR treatment resemble, in a remarkable manner, those caused by chromosomal instability,[41] a type of genomic instability that refers to the high rate by which chromosome structure and number changes over time in cancer cells compared with normal cells.[1] In this scenario, sustained JNK activation is also restricted to delaminated cells, and delaminated cells are the ones with the highest levels of aneuploidy in the tissue.[41] We would like, thus, to propose that segmental aneuploidy (in the case of IR-treated tissues) or whole-chromosome aneuploidy (in the case of chromosomal instability[41]) cause an imbalance in the expression levels of a large set of genes and, this imbalance well known to cause proteotoxic and metabolic stress in human and yeast cells,[42,43] induces JNK-dependent programmed cell death. When programmed cell death is blocked, a subversive tumorigenic role of JNK is unveiled. Whether this imbalance also contributes to the role of genomic instability in human cancer remains to be elucidated.

HR repair of DSBs also has a suppressor role of spontaneous tumor development in aged adult flies. Genome rearrangements, including translocations and deletions, are the most predominant type of mutations in aged adult flies,[44] and aged flies develop tumors in proliferating tissues such as the testis and the gut.[45] Impairment of HR repair, in flies mutant for *DmBlm* (the Drosophila ortholog of Bloom (BLM) RecQ helicase involved in unwinding the DNA double helix for replication or repair[46]), increases the frequency of genome rearrangements and, most interestingly, increases the frequency of tumor development at early ages in testis and gut tissues.[47] The incidence of genomic instability and spontaneous tumorigenesis in aged adult flies is largely unaffected by mutations in *lig4*.[47] Thus, genomic instability, in the form of chromosome rearrangements, also contributes to spontaneous tumor development in proliferative tissues of aged flies. These results together with the ones presented in the present work support the proposed tumorigenic role of genomic instability in human cancer.[48]

MATERIALS AND METHODS

Drosophila strains

UAS–mei-41^{RNAi} (ID 11251* and ID 103624, Vienna Drosophila RNAi Center (VDRC), Vienna, Austria); *UAS–okra^{RNAi}* (ID 104323*, VDRC and HMS00585 TRiP); *UAS–grapes^{RNAi}* (ID 12680* and ID 110076, VDRC); *UAS-spnA^{RNAi}* (ID 13362* and ID 14021, VDRC); *UAS- bsk^{K53R}* [*UAS-bsk^{DN}* in the text]*; UAS-p35; UAS-tribbles* (a kind gift from B Edgar); *UAS-dacapo* (a kind gift from I Hariharan); *viking (collagen IV)-GFP*;[12] *Df(3 L)H99; lig4^{169}*; *puckered-lacZ*[49] are described in Flybase.; *UAS-DE-CadΔCyt:α-Catenin*.[26] Other stocks are described in Flybase. dsRNA forms used in the main figures are the ones whose IDs contain an asterisk.

Immunohistochemistry

Mouse anti-MMP1 (14A3D2, Developmental Studies Hybridoma Bank (DSHB), Iowa City, IA, USA); rabbit anti-p35 (IMG5740, IMGENEX, San Diego, CA, USA); rabbit anti-gal (Cappel, Westchester, PA, USA); rat anti-Ci (2A1, DSHB); mouse anti-Fasciclin III (7G10, DSHB); mouse anti-disc large (4F3, DSHB); mouse anti-Wg (4D4, DSHB); rat anti-E-cadherin (DCAD2, DSHB); rabbit anti-atypical protein kinase C (DSHB); rabbit anti-laminin- (ab47651, AbCam, Cambridge, MA, USA); rabbit anti-P-H2AV (Rockland, Gilbertsville, PA, USA); and rabbit anti-human cleaved caspase 3 (Cell Signaling, Danvers, MA, USA). Secondary antibodies were obtained from Molecular Probes (Eugene, OR, USA).

Quantification of tissue growth

Size of the A and P compartments in the wing primordia were measured using the Fiji Software (NIH, Bethesda, MD, USA). At least 10 wing discs per genotype and condition were scored. The average P/A ratio and the corresponding s.d. were calculated and *t*-test analysis was carried out. In each experiment, control wing primordia (expressing p35 alone and subject or not to IR) were dissected and stained and the P/A ratio quantified. All genotypes included in each histogram were analyzed in parallel.

Mosaic analysis with a repressible cell marker clones

The following genotypes were used to generate loss-of-function clones for the H99 deficiency by the mosaic analysis with a repressible cell marker (Lee and Luo, 2001)[50] technique to simultaneously express different UAS transgenes in the clones: *hs-FLP, tub-Gal4, UAS-GFP/+; FRT2A tub-Gal80/ FRT2A Df(H99)*.

IR treatments

Irradiations were carried out in an YXLON MaxiShot X-ray system at the standard dose of 40 Gy. Clones of cells mutant for the H99 deficiency (*Df (H99)*) were induced by heat shock (1 h at 37 °C) at 72 h After egg laying (AEL), larvae were irradiated 24 h after clone induction and collected for dissection 72–96 h after IR treatment.

CONFLICT OF INTEREST

The authors declare no conflict of interest.

ACKNOWLEDGEMENTS

We thank B Edgar and I Hariharan for flies and reagents, T Yates for help in editing the manuscript, and M Clemente-Ruiz for comments on the manuscript. AD is funded by a Juan de la Cierva post-doctoral contract and LB by a pre-doctoral fellowship (Ministerio de Economía y Competitividad), MM is an ICREA Research Professor and MM's laboratory was funded by Grants from the Ministerio de Economía y Competitividad (BFU2010-21123 and CSD2007-00008), the Generalitat de Catalunya (2005 SGR 00118), intramural funds and the EMBO Young Investigator Programme.

REFERENCES

1 Negrini S, Gorgoulis VG, Halazonetis TD. Genomic instability–an evolving hallmark of cancer. *Nat Rev Mol Cell Biol* 2010; **11**: 220–228.
2 Lane D, Levine A. p53 Research: the past thirty years and the next thirty years. *Cold Spring Harb Perspect Biol* 2010; **2**: a000893.
3 Halazonetis TD, Gorgoulis VG, Bartek J. An oncogene-induced DNA damage model for cancer development. *Science* 2008; **319**: 1352–1355.
4 Jackson SP, Bartek J. The DNA-damage response in human biology and disease. *Nature* 2009; **461**: 1071–1078.
5 Foster SS, De S, Johnson LK, Petrini JH, Stracker TH. Cell cycle- and DNA repair pathway-specific effects of apoptosis on tumor suppression. *Proc Natl Acad Sci USA* 2012; **109**: 9953–9958.
6 Liu G, Parant JM, Lang G, Chau P, Chavez-Reyes A, El-Naggar AK *et al.* Chromosome stability, in the absence of apoptosis, is critical for suppression of tumorigenesis in Trp53 mutant mice. *Nat Genet* 2004; **36**: 63–68.
7 Brady CA, Jiang D, Mello SS, Johnson TM, Jarvis LA, Kozak MM *et al.* Distinct p53 transcriptional programs dictate acute DNA-damage responses and tumor suppression. *Cell* 2011; **145**: 571–583.
8 Valente LJ, Gray DH, Michalak EM, Pinon-Hofbauer J, Egle A, Scott CL *et al.* p53 efficiently suppresses tumor development in the complete absence of its cell-cycle inhibitory and proapoptotic effectors p21, Puma, and Noxa. *Cell reports* 2013; **3**: 1339–1345.
9 Brumby AM, Richardson HE. Scribble mutants cooperate with oncogenic Ras or Notch to cause neoplastic overgrowth in Drosophila. *EMBO J* 2003; **22**: 5769–5779.
10 Dar AC, Das TK, Shokat KM, Cagan RL. Chemical genetic discovery of targets and anti-targets for cancer polypharmacology. *Nature* 2012; **486**: 80–84.
11 Ohsawa S, Sato Y, Enomoto M, Nakamura M, Betsumiya A, Igaki T. Mitochondrial defect drives non-autonomous tumour progression through Hippo signalling in Drosophila. *Nature* 2012; **490**: 547–551.
12 Pagliarini RA, Xu T. A genetic screen in Drosophila for metastatic behavior. *Science* 2003; **302**: 1227–1231.
13 Song YH. Drosophila melanogaster: a model for the study of DNA damage checkpoint response. *Mol Cells* 2005; **19**: 167–179.
14 Brodsky MH, Nordstrom W, Tsang G, Kwan E, Rubin GM, Abrams JM. Drosophila p53 binds a damage response element at the reaper locus. *Cell* 2000; **101**: 103–113.
15 Peters M, DeLuca C, Hirao A, Stambolic V, Potter J, Zhou L *et al.* Chk2 regulates irradiation-induced, p53-mediated apoptosis in Drosophila. *Proc Natl Acad Sci USA* 2002; **99**: 11305–11310.

© 2015 Macmillan Publishers Limited

16 Song YH, Mirey G, Betson M, Haber DA, Settleman J. The Drosophila ATM ortholog, dATM, mediates the response to ionizing radiation and to spontaneous DNA damage during development. *Curr Biol* 2004; **14**: 1354–1359.
17 Jaklevic BR, Su TT. Relative contribution of DNA repair, cell cycle checkpoints, and cell death to survival after DNA damage in Drosophila larvae. *Curr Biol* 2004; **14**: 23–32.
18 Staeva-Vieira E, Yoo S, Lehmann R. An essential role of DmRad51/SpnA in DNA repair and meiotic checkpoint control. *EMBO J* 2003; **22**: 5863–5874.
19 Kooistra R, Vreeken K, Zonneveld JB, de Jong A, Eeken JC, Osgood CJ *et al.* The Drosophila melanogaster RAD54 homolog, DmRAD54, is involved in the repair of radiation damage and recombination. *Mol Cell Biol* 1997; **17**: 6097–6104.
20 Romeijn RJ, Gorski MM, van Schie MA, Noordermeer JN, Mullenders LH, Ferro W *et al.* Lig4 and rad54 are required for repair of DNA double-strand breaks induced by P-element excision in Drosophila. *Genetics* 2005; **169**: 795–806.
21 Hay BA, Wolff T, Rubin GM. Expression of baculovirus P35 prevents cell death in Drosophila. *Development* 1994; **120**: 2121–2129.
22 Perez-Garijo A, Martin FA, Morata G. Caspase inhibition during apoptosis causes abnormal signalling and developmental aberrations in Drosophila. *Development* 2004; **131**: 5591–5598.
23 Warner SJ, Yashiro H, Longmore GD. The Cdc42/Par6/aPKC polarity complex regulates apoptosis-induced compensatory proliferation in epithelia. *Curr Biol* 2010; **20**: 677–686.
24 Igaki T, Pagliarini RA, Xu T. Loss of cell polarity drives tumor growth and invasion through JNK activation in Drosophila. *Curr Biol* 2006; **16**: 1139–1146.
25 Uhlirova M, Bohmann D. JNK- and Fos-regulated Mmp1 expression cooperates with Ras to induce invasive tumors in Drosophila. *EMBO J* 2006; **25**: 5294–5304.
26 Pacquelet A, Rorth P. Regulatory mechanisms required for DE-cadherin function in cell migration and other types of adhesion. *J Cell Biol* 2005; **170**: 803–812.
27 Srivastava A, Pastor-Pareja JC, Igaki T, Pagliarini R, Xu T. Basement membrane remodeling is essential for Drosophila disc eversion and tumor invasion. *Proc Natl Acad Sci USA* 2007; **104**: 2721–2726.
28 Beaucher M, Hersperger E, Page-McCaw A, Shearn A. Metastatic ability of Drosophila tumors depends on MMP activity. *Dev Biol* 2007; **303**: 625–634.
29 Srivastava N, Gochhait S, de Boer P. Bamezai RN. Role of H2AX in DNA damage response and human cancers. *Mutat Res* 2009; **681**: 180–188.
30 Joyce EF, Pedersen M, Tiong S, White-Brown SK, Paul A, Campbell SD *et al.* Drosophila ATM and ATR have distinct activities in the regulation of meiotic DNA damage and repair. *J Cell Biol* 2011; **195**: 359–367.
31 Mata J, Curado S, Ephrussi A, Rorth P. Tribbles coordinates mitosis and morphogenesis in Drosophila by regulating string/CDC25 proteolysis. *Cell* 2000; **101**: 511–522.
32 Edgar BA, O'Farrell PH. Genetic control of cell division patterns in the Drosophila embryo. *Cell* 1989; **57**: 177–187.
33 Grosshans J, Wieschaus E. A genetic link between morphogenesis and cell division during formation of the ventral furrow in Drosophila. *Cell* 2000; **101**: 523–531.
34 Seher TC, Leptin M. Tribbles a cell-cycle brake that coordinates proliferation and morphogenesis during Drosophila gastrulation. *Curr Biol* 2000; **10**: 623–629.
35 Reis T, Edgar BA. Negative regulation of dE2F1 by cyclin-dependent kinases controls cell cycle timing. *Cell* 2004; **117**: 253–264.
36 de Nooij JC, Letendre MA, Hariharan IK. A cyclin-dependent kinase inhibitor, Dacapo, is necessary for timely exit from the cell cycle during Drosophila embryogenesis. *Cell* 1996; **87**: 1237–1247.
37 Lane ME, Sauer K, Wallace K, Jan YN, Lehner CF, Vaessin H. Dacapo a cyclin-dependent kinase inhibitor, stops cell proliferation during Drosophila development. *Cell* 1996; **87**: 1225–1235.
38 Li T, Kon N, Jiang L, Tan M, Ludwig T, Zhao Y *et al.* Tumor suppression in the absence of p53-mediated cell-cycle arrest, apoptosis, and senescence. *Cell* 2012; **149**: 1269–1283.
39 McVey M, Larocque JR, Adams MD, Sekelsky JJ. Formation of deletions during double-strand break repair in Drosophila DmBlm mutants occurs after strand invasion. *Proc Natl Acad Sci USA* 2004; **101**: 15694–15699.
40 McVey M, Adams M, Staeva-Vieira E, Sekelsky JJ. Evidence for multiple cycles of strand invasion during repair of double-strand gaps in Drosophila. *Genetics* 2004; **167**: 699–705.
41 Dekanty A, Barrio L, Muzzopappa M, Auer H, Milan M. Aneuploidy-induced delaminating cells drive tumorigenesis in Drosophila epithelia. *Proc Natl Acad Sci USA* 2012; **109**: 20549–20554.
42 Oromendia AB, Dodgson SE, Amon A. Aneuploidy causes proteotoxic stress in yeast. *Genes Dev* 2012; **26**: 2696–2708.
43 Stingele S, Stoehr G, Peplowska K, Cox J, Mann M, Storchova Z. Global analysis of genome, transcriptome and proteome reveals the response to aneuploidy in human cells. *Mol Syst Biol* 2012; **8**: 608.
44 Garcia AM, Calder RB, Dolle ME, Lundell M, Kapahi P, Vijg J. Age- and temperature-dependent somatic mutation accumulation in Drosophila melanogaster. *PLoS Genet* 2010; **6**: e1000950.
45 Salomon RN, Jackson FR. Tumors of testis and midgut in aging flies. *Fly (Austin)* 2008; **2**: 265–268.
46 Kusano K, Johnson-Schlitz DM, Engels WR. Sterility of Drosophila with mutations in the Bloom syndrome gene--complementation by Ku70. *Science* 2001; **291**: 2600–2602.
47 Garcia AM, Salomon RN, Witsell A, Liepkalns J, Calder RB, Lee M *et al.* Loss of the bloom syndrome helicase increases DNA ligase 4-independent genome rearrangements and tumorigenesis in aging Drosophila. *Genome Biol* 2011; **12**: R121.
48 Hanahan D, Weinberg RA. Hallmarks of cancer: the next generation. *Cell* 2011; **144**: 646–674.
49 Martin-Blanco E, Gampel A, Ring J, Virdee K, Kirov N, Tolkovsky AM *et al.* puckered encodes a phosphatase that mediates a feedback loop regulating JNK activity during dorsal closure in Drosophila. *Genes Dev* 1998; **12**: 557–570.
50 Lee T, Luo L Mosaic analysis with a repressible cell marker (MARCM) for Drosophila neural development. *Trends Neurosci* 2001; **24**: 251–254.

Supplementary Information accompanies this paper on the Oncogene website (http://www.nature.com/onc)

© 2015 Macmillan Publishers Limited